



Persistent Current, Magnetic Susceptibility, and Thermal Properties for a Class of Yukawa Potential in the Presence of External Magnetic and Aharonov–Bohm Fields

C. O. Edet¹ · A. N. Ikot¹ · U. S. Okorie^{1,2} · G. J. Rampho³ · M. Ramantswana³ · R. Horchani⁴ · H. Abdullah⁵ · J. A. Vinasco⁶ · C. A. Duque⁶ · Abdel-Haleem Abdel-Aty^{7,8}

Received: 29 April 2021 / Accepted: 29 June 2021 / Published online: 6 July 2021
© The Author(s), under exclusive licence to Springer Science+Business Media, LLC, part of Springer Nature 2021

Abstract

Using the asymptotic iteration method, the class of Yukawa potential is investigated in the non-relativistic regime, taking into account the influence of magnetic and Aharonov–Bohm flux fields. The system's energy equation and wave function are computed in compact form. The effect of the fields on the system's energy spectra is studied in depth. The presence of external magnetic and Aharonov–Bohm fields eliminates degeneracy from the system's energy spectrum. The partition function is determined using the energy equation, and it is then used to evaluate thermodynamic and magnetic properties of the system, such as persistent current and magnetic susceptibility.

Keywords Asymptotic iteration method · Magnetic and Aharonov–Bohm fields · Magnetic properties · Thermal properties

✉ A. N. Ikot
ndemikotphysics@gmail.com

¹ Theoretical Physics Group, Department of Physics, University of Port Harcourt, Choba, Nigeria

² Department of Physics, Akwa Ibom State University, Ikot Akpaden, P.M.B. 1167, Uyo, Nigeria

³ Department of Physics, University of South Africa, Florida, Johannesburg 1710, South Africa

⁴ Department of Physics, College of Science, Sultan Qaboos University, Al-Khod, P.O. Box 36, P.C. 123 Muscat, Sultanate of Oman

⁵ Physics Education Department, Faculty of Education, Tishk International University, Erbil 44001, Iraq

⁶ Grupo de Materia Condensada-UdeA, Instituto de Física, Facultad de Ciencias Exactas y Naturales, Universidad de Antioquia UdeA, Calle 70 No. 52-21, Medellín, Colombia

⁷ Department of Physics, College of Sciences, University of Bisha, P.O. Box 344, Bisha 61922, Saudi Arabia

⁸ Physics Department, Faculty of Science, Al-Azhar University, Assiut 71524, Egypt

1 Introduction

The Schrödinger equation (SE) is a fundamental equation in quantum mechanics (QM). This is because it is the equation that defines a particle's action in a microscopic setting. The solutions of SE with a given central potential have a wide variety of applications. Furthermore, several researchers have proposed that the SE's eigen-solutions (eigenvalues and eigenfunction) provide important knowledge about the quantum system [1–10]. Many studies of SE solutions with a variety of QM possible models have been published in the literature [11–14]. The class of Yukawa Potential (CYP) is one of the potentials. Onate and Ojonubah [15] were the first to suggest this model. Since it is a generalization of the Yukawa, Hellmann, Coulomb, and Inverse quadratic Yukawa potentials [15, 16], this atomic model is important. CYP has a wide range of uses in other areas of physics, including high-energy physics, atomic physics, and solid-state physics [16, 17]. The CYP can be written as [15]:

$$V(r) = -\frac{V_0 e^{-2\alpha r}}{r^2} - \frac{V_1}{r} + \frac{V_2 e^{-\alpha r}}{r}, \quad (1)$$

where r is the inter-particle distance, V_0 , V_1 , and V_3 are the potential parameters and α is the screening parameter which characterize the range of the interaction [15, 16].

In this research, we are interested in providing answers to the following questions: (i) what happens to the energy spectra of this model in the presence of the all-inclusive effect of magnetic and Aharonov–Bohm (AB) fields? (ii) What happens when there is a solitary effect? and (iii) What happens to its thermal and magnetic properties in the presence of this fields? This questions motivated us to carry out this study. Many researchers have recently concentrated their efforts on studies that look at the impact of magnetic and AB fields on the energy spectra and thermal properties of different potentials. Edet *et al.* [18] used the Nikiforov–Uvarov-Functional Analysis (NUFA) approach to solve the SE with Hellmann potential in the presence of external magnetic and AB flux fields. According to the authors, the AB field eliminates degeneracy more effectively than the magnetic field. Rampho *et al.* [19] used non-relativistic quantum mechanics to investigate the increased screened Kratzer potential (ISKP) in the presence of external magnetic and AB fields. Ikot *et al.* [20] used the factorization approach to solve the SE with the screened Kratzer potential (SKP) in the presence of magnetic and AB fields. The system's magnetic and other thermal properties were investigated. Ikot *et al.* [21] used the superstatistics formalism to examine the thermal properties of pseudo-harmonic potential in the presence of magnetic and AB fields for chosen diatomic molecules, and several experiments [22–36] have investigated the thermodynamic properties for various physical structures in recent times.

Jia *et al.* [37–42] have presented predictive studies of thermodynamic properties in diatomic molecules and gaseous substances, in carbonyl, and hydrogen sulfide and in carbon dioxide; Their studies have also included simulations of the ideal-gas thermodynamic properties for water. They have obtained excellent agreement between the calculated values and experimental data without needing to use an appreciable number of experimental spectroscopy parameters in their models. The

average relative deviations of their calculated values for the thermodynamical properties from the National Institute of Standards and Technology database over a wide temperature range are appreciably small. Essentially, their models have been based on the minimization of the Gibbs free energy of the system. In the same direction of research, Servatkah *et al.* [43] have studied the thermodynamic functions of H_2 and LiH . In their study, the Schrödinger equation was analytically solved with the generalized Morse potential using the Nikiforov–Uvarov method and considering the constant and the position-dependent effective mass models. They found that their theoretical findings of the thermodynamic functions are in agreement with experimental data when the generalized Morse potential includes the position-dependent effective mass model.

Our goal in this paper is to use the asymptotic iteration method (AIM) to solve the SE with the CYP model in the presence of magnetic and AB flux fields, and then use the obtained energy to measure the partition function and other thermodynamic functions including entropy, mean energy, free energy, specific heat capacity, magnetization, and magnetic susceptibility. The effects of the fields on the energy spectra, as well as the system's thermal and magnetic properties, will be discussed. The following is a breakdown of the paper's structure. In Sect. 2, we present our theoretical framework which is divided in two subsections where the first one is devoted to the solution of the SE with a CYP that takes AB flux and magnetic fields into account and in the second one we present the implications of the control parameter on the thermodynamic properties in the presence of the external fields. The discussions of results are presented in Sect. 3. Finally, a brief concluding remarks is given in Sect. 4.

2 Theoretical Framework

2.1 Schrödinger Equation with Class of Yukawa Potential Under Aharanov–Bohm and Magnetic Fields

In cylindrical coordinates, the Schrödinger equation of a charged particle confined by CYP under the combined effect of AB flux and external magnetic fields can be written as [18–36, 44]:

$$\left[\frac{1}{2\mu} \left(i\hbar \vec{\nabla} - \frac{e}{c} \vec{A} \right)^2 - \frac{V_0 e^{-2ar}}{r^2} - \frac{V_1}{r} + \frac{V_2 e^{-ar}}{r} \right] \psi(r, \varphi) = E_{nm} \psi(r, \varphi), \quad (2)$$

where E_{nm} denotes the energy level and μ is the effective mass of the system. The vector potential which is denoted by \vec{A} can be written as a superposition of two terms $\vec{A} = \vec{A}_1 + \vec{A}_2$ having the azimuthal components [47] and external magnetic field with $\vec{\nabla} \times \vec{A}_1 = \vec{B}$, $\vec{\nabla} \times \vec{A}_2 = 0$, where \vec{B} is the magnetic field. Here $\vec{A}_1 = \frac{Be^{-ar}}{(1-e^{-ar})} \hat{\varphi}$ and $\vec{A}_2 = \frac{\phi_{AB}}{2\pi r} \hat{\varphi}$ represents the additional magnetic flux ϕ_{AB} created by a solenoid with $\vec{\nabla} \cdot \vec{A}_2 = 0$ [18–36, 44]. The full vector potential is written in a simple form as [18, 44]

$$\vec{A} = \left(0, \frac{Be^{-\alpha r}}{(1 - e^{-\alpha r})} + \frac{\phi_{AB}}{2\pi r}, 0 \right). \quad (3)$$

Let us take a wave function in the polar coordinates as $\psi(r, \varphi) = \frac{1}{\sqrt{2\pi r}} e^{im\varphi} \rho_{nm}(r)$, where m denotes the magnetic quantum number. Inserting this wave function and the vector potential into Eq. 2, we arrive to the following radial second-order differential equation:

$$\begin{aligned} \rho_{nm}''(r) + \frac{2\mu}{\hbar^2} \left[E_{nm} + \frac{V_0 e^{-2\alpha r}}{r^2} + \frac{V_1}{r} - \frac{V_2 e^{-\alpha r}}{r} - \hbar\omega_c(m + \xi) \frac{e^{-\alpha r}}{(1 - e^{-\alpha r})r} \right. \\ \left. - \left(\frac{\mu\omega_c^2}{2} \right) \frac{e^{-2\alpha r}}{(1 - e^{-\alpha r})^2} - \frac{\hbar^2 \eta_m}{2\mu r^2} \right] \rho_{nm}(r) \\ = 0, \end{aligned} \quad (4)$$

where $\eta_m = (m + \xi)^2 - \frac{1}{4}$, $\xi = \frac{\phi_{AB}}{\phi_0}$ is an integer with the flux quantum $\phi_0 = \frac{hc}{e}$, and $\omega_c = \frac{eB}{\mu c}$ denotes the cyclotron frequency.

The Eq. 4 is not exactly solvable due to the presence of the r^{-2} centrifugal term. Therefore, we employ the Greene and Aldrich approximation scheme [45] to overcome the centrifugal term. This approximation is given by

$$\frac{1}{r^2} = \frac{\alpha^2}{(1 - e^{-\alpha r})^2}. \quad (5)$$

We point out here that this approximation is only valid for small values of the α screening parameter. If we consider the approximation above given by Eq. 5 combined with the transformation $s = e^{-\alpha r}$, the Eq. 4 can be rewritten as follows:

$$\begin{aligned} \rho_{nm}''(s) + \frac{\rho_{nm}'(s)}{s} \\ + \frac{[-(\epsilon_{nm} - P_0 - P_2 + P_4)s^2 + (2\epsilon_{nm} - P_1 - P_2 - P_3)s - (\epsilon_{nm} - P_1 + \eta_m)] \rho_{nm}(s)}{(s(1-s))^2} \\ = 0, \end{aligned} \quad (6)$$

where $\epsilon_{nm} = -\frac{2\mu E_{nm}}{\hbar^2 \alpha^2}$, $P_0 = \frac{2\mu V_0}{\hbar^2}$, $P_1 = \frac{2\mu V_1}{\hbar^2 \alpha}$, $P_2 = \frac{2\mu V_2}{\hbar^2 \alpha}$, $P_3 = \frac{2\mu \omega_c}{\hbar \alpha} (m + \xi)$, and $P_4 = \left(\frac{\mu \omega_c}{\hbar \alpha} \right)^2$.

We assume a wave function $\rho_{nm}(s)$ to be of the form

$$\rho_{nm}(s) = s^\lambda (1-s)^{\sigma_m} y_{nm}(s), \quad (7)$$

where

$$\sigma_m = \frac{1}{2} + \sqrt{(m + \xi)^2 - \frac{2\mu V_0}{\hbar^2} + \left(\frac{\mu \omega_c}{\hbar \alpha} \right)^2 + \frac{2\mu \omega_c}{\hbar \alpha} (m + \xi)} \quad (8)$$

and

$$\lambda = \sqrt{\epsilon_{nm} - P_1 + \eta_m}. \tag{9}$$

Substituting Eq. 7 into Eq. 6 gives the following equation:

$$y''_{nm}(s) = \frac{[(2\lambda + 2\sigma_m + 1)s - (2\lambda + 1)]}{s(1 - s)} y'_{nm}(s) + \frac{[(\lambda + \sigma_m)^2 - (\sqrt{\epsilon_{nm} - P_0 - P_2 + P_4})^2]}{s(1 - s)} y_{nm}(s). \tag{10}$$

The Eq. 10 is a second-order homogeneous linear differential equation, which can be solved using the well-known asymptotic iteration method [46]. Rewriting Eq. 10 in the following form [47] to begin the methodical methodology of the AIM:

$$y''_{nm}(s) - \lambda_0(s)y_{nm}(s) - s_0(s)y_{nm}(s) = 0, \tag{11}$$

where

$$\lambda_0(s) = \frac{[(2\lambda + 2\sigma_m + 1)s - (2\lambda + 1)]}{s(1 - s)} \tag{12}$$

and

$$s_0(s) = \frac{[(\lambda + \sigma_m)^2 - (\sqrt{\epsilon_{nm} - P_0 - P_2 + P_4})^2]}{s(1 - s)}. \tag{13}$$

The primes of the function $y_{nm}(s)$ in Eq. 11 means the derivatives with respect to s . The asymptotic feature of the method for sufficiently large k is given as [46, 47]

$$\frac{s_k(s)}{\lambda_k(s)} = \frac{s_{k-1}(s)}{\lambda_{k-1}(s)} = \alpha(s), \tag{14}$$

where

$$\lambda_k(s) = \lambda'_{k-1}(s) + s_{k-1}(s) + \lambda_0(s)\lambda_{k-1}(s) \tag{15}$$

and

$$s_k(s) = s'_{k-1}(s) + s_0(s)\lambda_{k-1}(s). \tag{16}$$

The recurrence relations [46, 47] are established by Eqs. 15, 16. The equation we search can be derived from the roots of the following equation using the asymptotic iteration method [46, 47]

$$\delta_k(s) = \begin{vmatrix} \lambda_k(s) & s_k(s) \\ \lambda_{k+1}(s) & s_{k+1}(s) \end{vmatrix} = 0, \quad \text{where } k = 1, 2, 3 \dots \tag{17}$$

Thus, we can easily obtain the following simple arithmetic progressions:

$$\delta_0(s) = \left| \begin{matrix} \lambda_0(s) & s_0(s) \\ \lambda_1(s) & s_1(s) \end{matrix} \right| = 0 \Leftrightarrow \lambda_0 = -0 - \sigma_m \pm \sqrt{\varepsilon_{nm} - P_0 - P_2 + P_4}, \quad (18)$$

$$\delta_1(s) = \left| \begin{matrix} \lambda_1(s) & s_1(s) \\ \lambda_2(s) & s_2(s) \end{matrix} \right| = 0 \Leftrightarrow \lambda_1 = -1 - \sigma_m \pm \sqrt{\varepsilon_{nm} - P_0 - P_2 + P_4}, \quad (19)$$

and

$$\delta_2(s) = \left| \begin{matrix} \lambda_2(s) & s_2(s) \\ \lambda_3(s) & s_3(s) \end{matrix} \right| = 0 \Leftrightarrow \lambda_2 = -2 - \sigma_m \pm \sqrt{\varepsilon_{nm} - P_0 - P_2 + P_4}, \text{ etc.} \quad (20)$$

By considering the finiteness of the solutions, the quantum condition is given by

$$\lambda_n = -n - \sigma_m \pm \sqrt{\varepsilon_{nm} - P_0 - P_2 + P_4}, \quad (21)$$

from which we obtain

$$\varepsilon_{nm} = P_1 - \eta_m + \frac{1}{4} \left(\frac{P_1 - P_2 - P_0 + P_4 - \eta_m - (n + \sigma_m)^2}{n + \sigma_m} \right)^2. \quad (22)$$

Hence, if one substitutes the value of the dimensionless parameters defined after Eq. 6 into Eq. 22, we obtain the solutions as follows:

$$E_{nm} = \frac{\hbar^2 \alpha^2 \eta_m}{2\mu} - V_1 \alpha - \frac{\hbar^2 \alpha^2}{8\mu} \times \left[\frac{\frac{2\mu V_1}{\hbar^2 \alpha} - \frac{2\mu V_2}{\hbar^2 \alpha} - \frac{2\mu V_0}{\hbar^2} + \left(\frac{\mu \omega_c}{\hbar \alpha} \right)^2 - \eta_m - (n + \sigma_m)^2}{n + \sigma_m} \right]^2. \quad (23)$$

We continue to find the system’s wave function for completeness’ sake. Let’s figure out what this system’s wave function is. In general, the differential equation we want to solve should be translated into a format that makes AIM [46, 47] easy to use

$$y''(x) = 2 \left(\frac{ax^{N+1}}{1 - bx^{N+2}} - \frac{M + 1}{x} \right) y'(x) - \frac{Wx^N}{1 - bx^{N+2}} y(x), \quad (24)$$

where a , b , and M are constants. The exact solutions for Eq. 24 is given by

$$y(x) = (-1)^n C(N + 2)^n (\sigma)_n {}_2F_1(-n, t + n; \sigma; bx^{N+2}), \quad (25)$$

where $(\sigma)_n = \frac{\Gamma(\sigma+n)}{\Gamma(\sigma)}$, $\sigma = \frac{2M+N+3}{N+2}$, and $t = \frac{(2M+1)b+2a}{(N+2)b}$.

By comparing Eq. 11 with Eq. 24, we can deduce that $M = \sigma_m - \frac{1}{2}$, $t = 2(\lambda + \sigma_m)$, $a = \sigma_m \sigma = 2\lambda + 1$, $b = 1$, $N = -1(\sigma_n) = \frac{\Gamma(2\lambda+1+n)}{\Gamma(2\lambda+1)}$ and

$$y_{nm}(s) = (-1)^n C_2 \frac{\Gamma(2\lambda + 1 + n)}{\Gamma(2\lambda + 1)} {}_2F_1(-n, 2(\lambda + \sigma_m) + n; 2\lambda + 1; s). \quad (26)$$

It is therefore straightforward to deduce that the corresponding unnormalized wave function is obtain as

$$R_{nm}(s) = (-1)^n C_2 \frac{\Gamma(2\lambda + 1 + n)}{\Gamma(2\lambda + 1)} s^\lambda (1 - s)^{\sigma_m} {}_2F_1(-n, 2(\lambda + \sigma_m) + n; 2\lambda + 1; s), \tag{27}$$

where C_2 is the normalization constant and ${}_2F_1(-n, 2(\lambda + \sigma_m) + n; 2\lambda + 1; s)$ is the hypergeometric function.

The particular case of the three-dimensional non-relativistic energy solutions are obtained by setting $m = \ell + \frac{1}{2}$, where $-\ell$ is the rotational quantum number, in Eq. 23 to obtain

$$E_{n\ell} = \frac{\hbar^2 \alpha^2 \ell(\ell + 1)}{2\mu} - V_1 \alpha - \frac{\hbar^2 \alpha^2}{8\mu} \times \left[\frac{\frac{2\mu V_1}{\hbar^2 \alpha} - \frac{2\mu V_2}{\hbar^2 \alpha} - \frac{2\mu V_0}{\hbar^2} - \ell(\ell + 1) - \left(n + \frac{1}{2} + \sqrt{\frac{1}{4} + \ell(\ell + 1) - \frac{2\mu V_0}{\hbar^2}} \right)^2}{\left(n + \frac{1}{2} + \sqrt{\frac{1}{4} + \ell(\ell + 1) - \frac{2\mu V_0}{\hbar^2}} \right)} \right]^2. \tag{28}$$

2.2 Thermo-magnetic Properties of Class of Yukawa Potential

It is well understood that the partition function of a system can be used to obtain all thermodynamic properties [48–51]. Easy summation over all vibrational energy levels available to the system can be used to calculate the vibrational partition function. Given the energy spectrum in Eq. 23, the partition function $Z(\beta)$ of the CYP at finite temperature, T , is obtained with the Boltzmann factor as [48];

$$Z(\beta) = \sum_{n=0}^{n_{max}} e^{-\beta E_n}, \tag{29}$$

where $\beta = \frac{1}{kT}$, with k the Boltzmann constant.

Substituting Eq. 23 in Eq. 29, we have

$$Z(\beta) = \sum_{n=0}^{n_{max}} e^{-\beta \left(Q_0 - Q_1 \left(\frac{Q_2 - (n + \sigma_m)^2}{(n + \sigma_m)} \right)^2 \right)}, \tag{30}$$

where n is the vibrational quantum number, $n = 0, 1, 2, 3 \dots n_{max}$. Here n_{max} denotes the upper bound vibration quantum number. We have introduced the following notations: $Q_0 = \frac{\hbar^2 \alpha^2 n_m}{2\mu} - V_1 \alpha$, $Q_1 = \frac{\hbar^2 \alpha^2}{8\mu}$, and $Q_2 = \frac{2\mu V_1}{\hbar^2 \alpha} - \frac{2\mu V_2}{\hbar^2 \alpha} - \frac{2\mu V_0}{\hbar^2} + \left(\frac{\mu \omega_c}{\hbar \alpha} \right)^2 - \eta_m$.

The maximum value n_{max} can be obtained by setting $\frac{dE_n}{dn} = 0$, i.e., $n_{max} = -\sigma_m \pm \sqrt{Q_2}$.

Replacing the summation in Eq. 30 by an integral, we have;

$$Z(\beta) = \int_0^{n_{max}} e^{-\beta \left(Q_0 - Q_1 \left(\frac{Q_2 - (n + \sigma_m)^2}{(n + \sigma_m)} \right)^2 \right)} dn. \tag{31}$$

If we set $x = \frac{Q_2}{(n + \sigma_m)} - (n + \sigma_m)$, we can rewrite the above integral in Eq. 31 as follows:

$$\begin{aligned} & \int_{x_1}^{x_2} e^{-\beta \left(Q_0 - Q_1 \left(\frac{Q_2 - (n + \sigma_m)^2}{(n + \sigma_m)} \right)^2 \right)} dx \\ &= \frac{1}{2} e^{-\beta Q_0} \int_{x_1}^{x_2} e^{\beta Q_1 x^2} \left(\frac{x}{\sqrt{x^2 + 4Q_2}} - 1 \right) dx, \end{aligned} \tag{32}$$

where $x_1 = \frac{Q_2}{\sigma_m} - \sigma_m$ and $x_2 = \frac{Q_2}{(n_{max} + \sigma_m)} - (n_{max} + \sigma_m)$.

On evaluating the integral in Eq. 32, we obtain the partition function of the CYP in magnetic and AB fields as follows

$$Z(\beta) = \frac{1}{2} e^{-\beta Q_0} \left[\frac{\frac{\sqrt{\pi} \left(\text{Erfi} \left[\sqrt{Q_1} x_1 \sqrt{\beta} \right] - \text{Erfi} \left[\sqrt{Q_1} x_2 \sqrt{\beta} \right] \right)}{2\sqrt{Q_1} \sqrt{\beta}} - e^{-4\beta Q_1 Q_2} \sqrt{\pi} \left(\text{Erfi} \left[\sqrt{Q_1} \sqrt{4Q_2 + x_1^2} \sqrt{\beta} \right] - \text{Erfi} \left[\sqrt{Q_1} \sqrt{4Q_2 + x_2^2} \sqrt{\beta} \right] \right)}{2\sqrt{Q_1} \sqrt{\beta}} \right]. \tag{33}$$

The classical partition function is represented by the previous Eq. 33. The explanation for this is that Eq. 33 lacks quantum corrections. The partition function in Eq. 33 can be used to obtain both thermal and magnetic properties of the CYP in the presence of the AB and magnetic fields, such as the free energy (F), entropy (S), mean energy (U), specific heat (C), magnetization (M), magnetic susceptibility (χ), and persistent current (I). The following expressions can be used to calculate the system’s thermodynamic functions [48–51]:

$$F(\beta) = -\frac{1}{\beta} \ln Z(\beta), \tag{34}$$

$$S(\beta) = \ln Z(\beta) - \beta \frac{d \ln Z(\beta)}{d\beta}, \tag{35}$$

$$U(\beta) = -\frac{d \ln Z(\beta)}{d\beta}, \tag{36}$$

$$C(\beta) = \beta^2 \frac{d^2 \ln Z(\beta)}{d\beta^2}, \tag{37}$$

$$M(\beta) = \frac{1}{\beta} \left(\frac{1}{Z(\beta)} \right) \left(\frac{\partial}{\partial B} Z(\beta) \right), \tag{38}$$

$$\chi_m(\beta) = \frac{\partial M(\beta)}{\partial B}, \tag{39}$$

and

$$I(\beta) = -\frac{e}{hc} \frac{\partial F(\beta)}{\partial \phi_{AB}}. \tag{40}$$

3 Discussion and Application of Results

In this section we present our main findings for the CYP energy structure given by Eq. 23 and the corresponding thermal properties obtained by Eqs. 34–40. For the units and main parameters we have used: $e = 1, h = 1, \hbar = 1, c = 1, \mu = 1, V_0 = 1, V_1 = 2, V_2 = 1, \alpha = 0.005$. All the energies will be in eV, the β -parameter in eV^{-1} , and the magnetic field in Teslas (T). We note that Eqs. 33–40 are presented as a function of the β -parameter which is equivalent to report the results a function of the temperature, T .

Table 1 shows the numerical energy values for the CYP under the influence of AB flux and magnetic fields with various values of magnetic and vibrational quantum numbers. We observe that when both fields are absent $B = \xi = 0$, there exist degeneracy in the energy spectra (note the same energy values for states with $m \pm 1$ and $n = 1$ and states with $m \pm 1$ and $n = 2$. Also states with $m \pm 1$ and $n = 3$ are very close in their energy values). By introducing only applied magnetic field ($B \neq 0, \xi = 0$) to the system, the energy eigenvalues is increased and bounded as

Table 1 Energy values (in eV) for the Class of Yukawa potential under the combined influence of the ξ -Aharanov–Bohm flux and B -magnetic fields with various values of the m -principal and n -vibrational quantum numbers

m	n	$B = 0, \xi = 0$	$B = 5, \xi = 0$	$B = 0, \xi = 5$	$B = 5, \xi = 5$
0	0	0.163822	- 0.0100042	- 0.0229687	- 0.0100415
	1	- 0.0143748	- 0.0100242	- 0.0184652	- 0.0101856
	2	- 0.0384761	- 0.0100691	- 0.0157032	- 0.0103542
	3	- 0.0325643	- 0.0101388	- 0.0138989	- 0.0105472
- 1	0	0.229206	- 0.0099968	- 0.0328492	- 0.0100341
	1	- 0.0658725	- 0.0099918	- 0.024119	- 0.0101534
	2	- 0.0567804	- 0.0100117	- 0.0192563	- 0.0102974
	3	- 0.0391438	- 0.0100566	- 0.016285	- 0.0104659
1	0	0.229206	- 0.0100117	- 0.0176456	- 0.0100489
	1	- 0.0658725	- 0.0100566	- 0.0150874	- 0.0102177
	2	- 0.0567804	- 0.0101263	- 0.0134145	- 0.0104108
	3	- 0.0391438	- 0.0102208	- 0.0122711	- 0.0106284

well. The presence of magnetic field takes away the degeneracy. The application of the AB field only ($B = 0$, $\xi \neq 0$), also lifts the degeneracy and the system is still bounded. The combined effect of both fields is robust and therefore, there is an upward shift in the bound state energy of the system. The combined effect shows that the system is highly attractive and bounded. The combined effects of AB flux and magnetic fields completely eliminates the degeneracy.

Figure 1 shows the plots of partition function of CYP in magnetic and AB fields: (a) versus β varying n_{max} , (b) versus B for varying β , and (c) versus ξ varying β . In Fig. 1a, the partition function increases with increasing β . Figure 1b shows that the partition function decreases and then increases with increasing magnetic field. Figure 1c shows that the partition function increases with increasing AB field. The partition function diverges if the distance $E_{n+1} - E_n$ between successive energy levels becomes smaller rather than larger as $n_{max} \rightarrow 0$. Then the later terms in the partition function $Z = \dots + e^{-(E_n - E_1)/kT} + e^{-(E_{n+1} - E_1)/kT} + e^{-(E_{n+2} - E_1)/kT} + \dots$, all start having about the same value since, if $\lim_{n \rightarrow \infty} (E_{n+1} - E_1) = 0$, the energy differences $E_n - E_1$ in the numerators of the Boltzmann factors all start having about the same value, i.e., you are adding infinitely many numbers that are all basically the same value and you will get divergence. An example would be the partition function over the infinitely many bound states of an atom like Hydrogen. The bound-state energy levels are given by $E_n = -13.6/n^2$ eV so the levels get closer and closer together as they all approach the limiting value E , which separates the bound states from the ionized (unbound) states. From the results in Fig. 1, it is concluded that the increase of the n_{max} and β parameters allow to reinforce the temperature, the magnetic field, and the ξ -parameter effects. It is clear from Fig. 1b that, the Z -function reaches saturation values for high magnetic field values, regardless of the β -parameter.

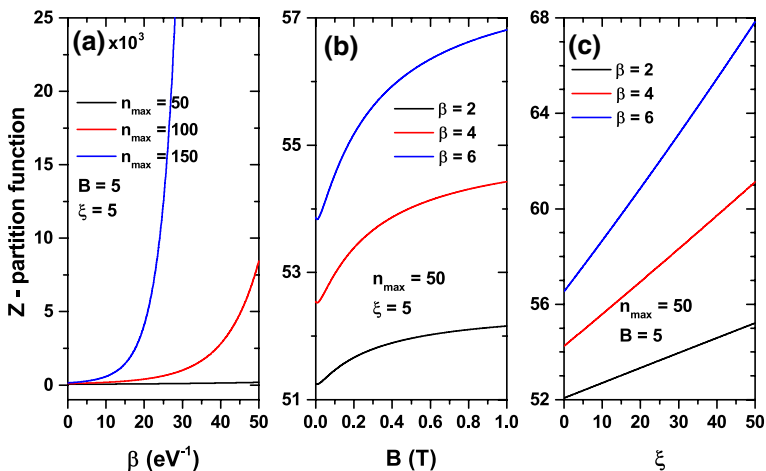


Fig. 1 Plots of partition function of Class of Yukawa potential in magnetic and Aharanov–Bohm fields: (a) versus β , varying n_{max} and keeping fixed the B and ξ parameters; (b) versus B , for varying β and keeping fixed the n_{max} and ξ parameters; and (c) versus ξ , varying β and keeping fixed the B and n_{max} parameters

Figure 2 shows the plots of free energy of CYP in magnetic and AB fields: (a) versus β varying n_{max} , (b) versus B for varying β , and (c) versus ξ varying β . In Fig. 2a, it can be seen that the free energy exhibits saturation. This means that as the β -Boltzmann factor increases, the free energy reach a limit. Figure 2b shows that the free energy increases with increasing magnetic field. Figure 2c shows that the free energy decreases with increasing AB field. The results in Fig. 2 show that the free energy is highly sensitive to changes in the n_{max} -parameter, slightly sensitive to the β -parameter, and essentially insensitive to the applied magnetic field changes. For $\beta \rightarrow 0$ the presence of the divergence in the free energy is associated with the almost zero value of the corresponding Z-function.

Figure 3 shows the plots of entropy of CYP in magnetic and AB fields: (a) versus β varying n_{max} , (b) versus B for varying β , and (c) versus ξ varying β . In Fig. 3a, the entropy decreases with increasing β . Figure 3b shows that the entropy increases with increasing magnetic field. Figure 3c shows that the entropy decreases with increasing AB field. The results in Fig. 3 allow us to infer that entropy is a function equally sensitive to temperature, the applied magnetic field, and the AB field, presenting the most important changes for high values of the n_{max} and β parameters. This shows the importance on the entropy of the highly excited states in the system.

Figure 4 shows the plots of mean energy of CYP in magnetic and AB fields: (a) versus β varying n_{max} , (b) versus B for varying β , and (c) versus ξ varying β . In Fig. 4a, the mean energy reduces with increasing β . Figure 4b shows that the mean energy increases and then slightly decreases with increasing magnetic field. Figure 4c shows that the mean energy decreases with increasing AB field. From the results in Fig. 4, it is inferred that mean energy is mostly sensitive to changes in the n_{max} parameter. Note the presence of the 10^{-2} global factor in Fig. 4b and c, which is associated with significantly small variations in the U -function.

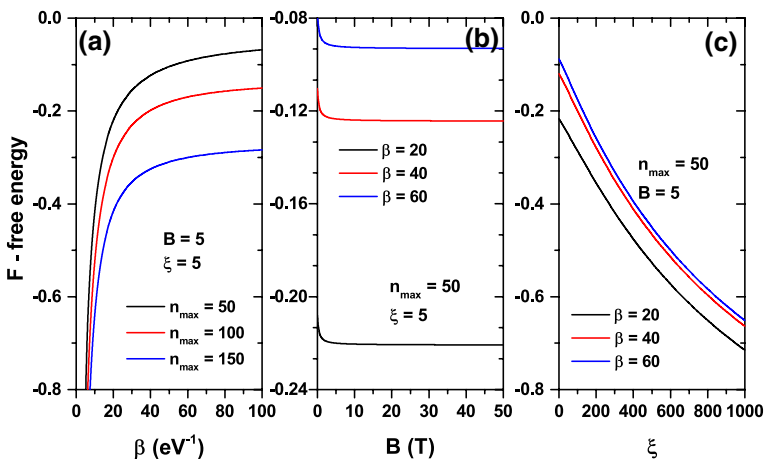


Fig. 2 Plots of the free energy of Class of Yukawa potential in magnetic and Aharanov–Bohm fields: (a) versus β , varying n_{max} and keeping fixed the B and ξ parameters; (b) versus B , for varying β and keeping fixed the n_{max} and ξ parameters; and (c) versus ξ , varying β and keeping fixed the B and n_{max} parameters

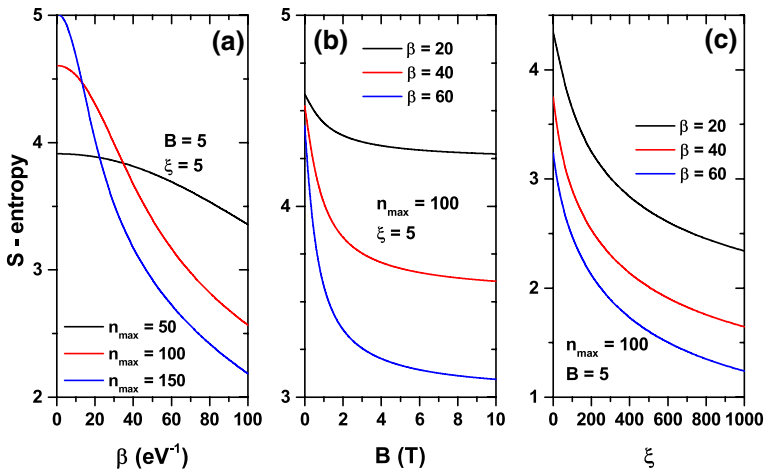


Fig. 3 Plots of the entropy of Class of Yukawa potential in magnetic and Aharanov–Bohm fields: (a) versus β , varying n_{max} and keeping fixed the B and ξ parameters; (b) versus B , for varying β and keeping fixed the n_{max} and ξ parameters; and (c) versus ξ , varying β and keeping fixed the B and n_{max} parameters

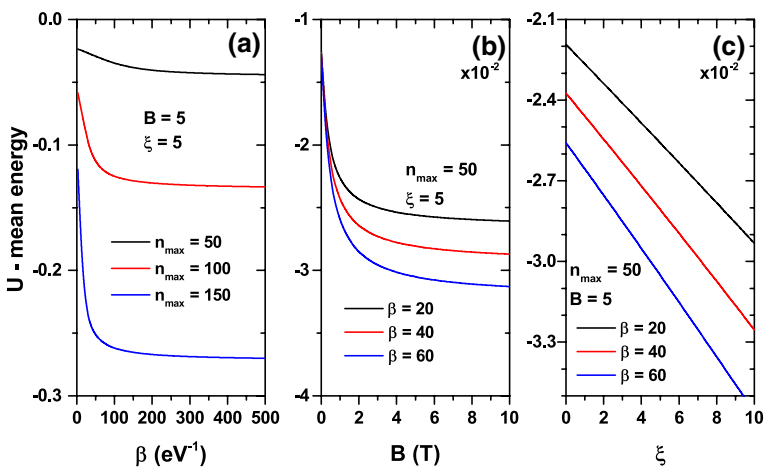


Fig. 4 Plots of the mean energy of Class of Yukawa potential in magnetic and Aharanov–Bohm fields: (a) versus β , varying n_{max} and keeping fixed the B and ξ parameters; (b) versus B , for varying β and keeping fixed the n_{max} and ξ parameters; and (c) versus ξ , varying β and keeping fixed the B and n_{max} parameters

Figure 5 shows the plots of specific heat capacity of CYP in magnetic and AB fields: (a) versus β varying n_{max} , (b) versus B for varying β , and (c) versus ξ varying β . In Fig. 5a, the specific heat capacity rises with increasing β . Figure 5b shows that the specific heat capacity decreases at the origin to almost zero-point and then increases again with increasing magnetic field. Figure 5c shows that the specific heat capacity increases with increasing AB field. From Fig. 5 it can be concluded that the

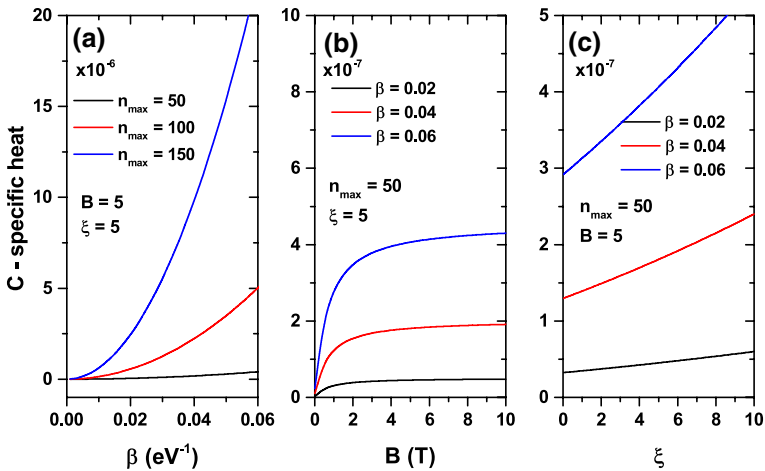


Fig. 5 Plots of the specific heat capacity of Class of Yukawa potential in magnetic and Aharanov–Bohm fields: (a) versus β , varying n_{max} and keeping fixed the B and ξ parameters; (b) versus B , for varying β and keeping fixed the n_{max} and ξ parameters; and (c) versus ξ , varying β and keeping fixed the B and n_{max} parameters

C -function is essentially insensitive to changes in temperature, in the applied magnetic field, and in the AB field. Note the presence of the 10^{-6} global factor in Fig. 5a and of the 10^{-7} factor in Fig. 5b and c.

Figure 6 shows the plots of magnetization of CYP in magnetic and AB fields: (a) versus β varying n_{max} , (b) versus B for varying β , and (c) versus ξ varying β . In Fig. 6a, the magnetization rises with increasing β . Figure 6b shows that the

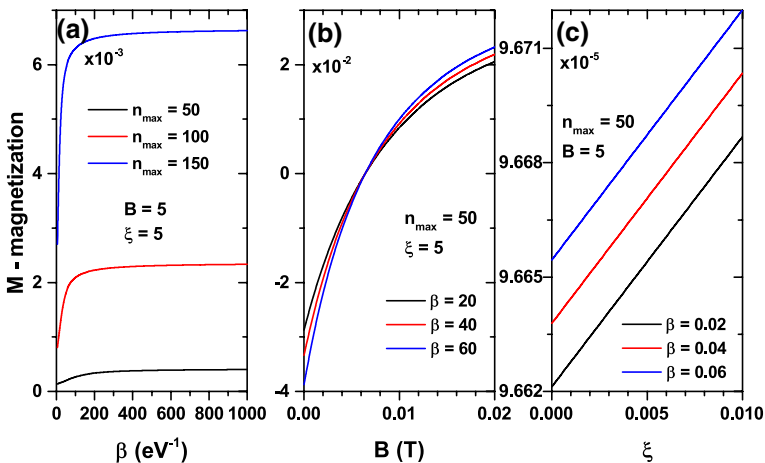


Fig. 6 Plots of the magnetization of Class of Yukawa potential in magnetic and Aharanov–Bohm fields: (a) versus β , varying n_{max} and keeping fixed the B and ξ parameters; (b) versus B , for varying β and keeping fixed the n_{max} and ξ parameters; and (c) versus ξ , varying β and keeping fixed the B and n_{max} parameters

magnetization increases with increasing magnetic field. The magnetization also pseudo-saturates as the magnetic tends to high values. Figure 6c shows that the magnetization increases linearly with increasing AB field. The results in Fig. 6 allow us to conclude that magnetization is mostly sensitive to changes in the applied magnetic field and is essentially constant for variations in the AB field.

Figure 7 shows the plots of magnetic susceptibility of CYP in magnetic and AB fields: (a) versus β varying n_{max} , (b) versus B for varying β , and (c) versus ξ varying β . In Fig. 7a, the magnetic susceptibility decreases with increasing β . Figure 7b shows that the magnetic susceptibility decreases with increasing magnetic field. Figure 7c shows that the magnetic susceptibility decreases linearly with increasing AB field. From Fig. 7 it can be concluded that the magnetic susceptibility shows its greatest changes in the presence of the applied magnetic field and that this effect is reinforced as the β -parameter increases. Note the presence of the 10^{-3} global factor of in Fig. 7a and 10^{-4} factor in Fig. 7b. In Fig. 7a it is observed that variations in magnetic susceptibility with temperature are significant in the high temperature regime and mainly in the large n_{max} range, that is, when there is a greater contribution of highly excited.

Figure 8 shows the plots of persistent current of CYP in magnetic and AB fields: (a) versus β varying n_{max} , (b) versus B for varying β , and (c) versus ξ varying β . In Fig. 8a, the persistent current increases with increasing β . Figure 8b shows that the persistent current increases with increasing magnetic field. The persistent current also saturates as the magnetic tends to high values. Figure 8c shows that the persistent current decreases linearly with increasing AB field. Fig. 8a shows that the most noticeable changes in persistent current occur for variations in the n_{max} parameter and that temperature has a significant effect on the high temperature regime, that is, when $\beta \rightarrow 0$.

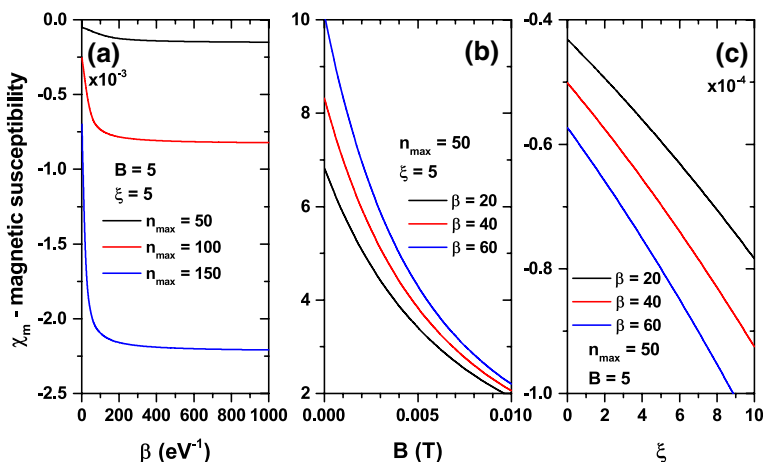


Fig. 7 Plots of the magnetic susceptibility of Class of Yukawa potential in magnetic and Aharanov–Bohm fields: (a) versus β , varying n_{max} and keeping fixed the B and ξ parameters; (b) versus B , for varying β and keeping fixed the n_{max} and ξ parameters; and (c) versus ξ , varying β and keeping fixed the B and n_{max} parameters

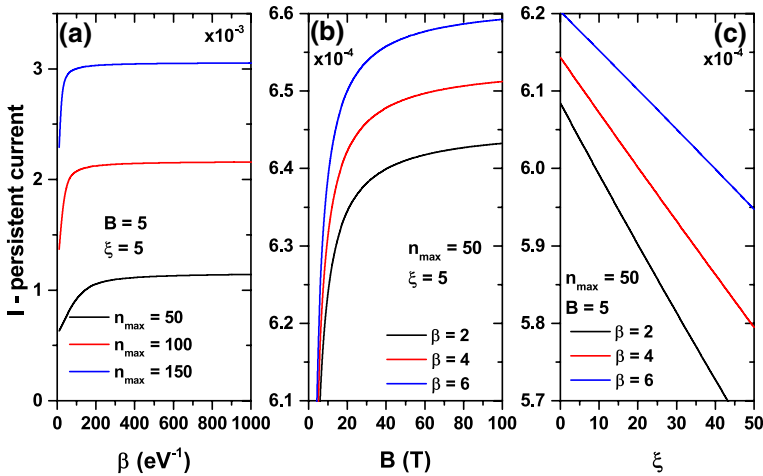


Fig. 8 Plots of the persistent current of Class of Yukawa potential in magnetic and Aharanov–Bohm fields: (a) versus β , varying n_{max} and keeping fixed the B and ξ parameters; (b) versus B , for varying β and keeping fixed the n_{max} and ξ parameters; and (c) versus ξ , varying β and keeping fixed the B and n_{max} parameters

4 Conclusions

In this paper, the CYP in the presence of external magnetic and AB flux fields is investigated. The Hamiltonian operator containing the vector potential and CYP is converted into a second-order differential equation. To obtain the energy equation and wave function of the system, we solve this differential equation using AIM. The effect of the fields on the system’s energy spectra is investigated in detail. The magnetic and AB fields were discovered to remove degeneracy. With the energy equation in hand, we calculated the partition function and used it to calculate the free energy, internal energy, entropy, specific heat capacity, magnetization, magnetic susceptibility, and persistent current, among other thermal and magnetic properties of the system. The magnetic susceptibility exhibits a diamagnetic behavior when plotted against β , paramagnetic when plotted against magnetic field, and again diamagnetic when plotted against AB field. This varying behavior of the magnetic susceptibility (where the system changes from paramagnetism to diamagnetism and vice versa) depends on the particular values of magnetic and AB fields values at which the observation are made. This may also have its origin in the changing confinement of the system. The findings of this research can be used in condensed matter physics, as well as atomic and molecular physics.

Acknowledgements CAD is grateful to the Colombian Agencies: CODI-Universidad de Antioquia (Estrategia de Sostenibilidad de la Universidad de Antioquia and projects “Efectos de capas delta dopadas en pozos cuánticos como fotodetectores en el infrarrojo”, “Propiedades magneto-ópticas y óptica no lineal en superredes de Grafeno”, “Efectos ópticos intersubbanda, no lineales de segundo orden y dispersión Raman, en sistemas asimétricos de pozos cuánticos acoplados”, and “Estudio de propiedades ópticas en sistemas semiconductores de dimensiones nanoscópicas”), and Facultad de Ciencias Exactas y

Naturales-Universidad de Antioquia (CAD exclusive dedication Project 2020-2021). CAD also acknowledges the financial support from *El Patrimonio Autónomo Fondo Nacional de Financiamiento para la Ciencia, la Tecnología y la Innovación Francisco José de Caldas* (Project: CD 111580863338, CT FP80740-173-2019).

References

1. C.O. Edet, U.S. Okorie, A.T. Ngiangia, A.N. Ikot, Bound state solutions of the Schrodinger equation for the modified Kratzer potential plus screened Coulomb potential. *Indian J. Phys.* **94**, 425–433 (2020)
2. L.D. Landau, E.M. Lifshitz, *Quantum Mechanics, Non-Relativistic Theory* (Pergamon Press, Oxford, 1977), p. 677
3. P.O. Okoi, C.O. Edet, T.O. Magu, Relativistic treatment of the Hellmann-generalized morse potential. *Rev. Mex. Fis.* **66**, 1–13 (2020)
4. L.I. Schiff, *Quantum Mechanics* (McGraw Hill, New York, 1968), p. 544
5. C.O. Edet, U.S. Okorie, G. Osobonye, A.N. Ikot, G.J. Rampho, R. Sever, Thermal properties of Deng-Fan-Eckart potential model using Poisson summation approach. *J. Math. Chem.* **58**, 989–1013 (2020)
6. W. Greiner, *Relativistic Quantum Mechanics: Wave Equations* (Springer, Berlin, 2000), p. 424
7. C.O. Edet, P.O. Okoi, Any 1-state solutions of the Schrödinger equation for q-deformed Hulthen plus generalized inverse quadratic Yukawa potential in arbitrary dimensions. *Rev. Mex. Fis.* **65**, 333–344 (2019)
8. U.S. Okorie, A.N. Ikot, C.O. Edet, G.J. Rampho, R. Sever, I.O. Akpan, Solutions of the Klein Gordon equation with generalized hyperbolic potential in D-dimensions, *J. Phys. Commun.* **3**, 095015 (2019)
9. P.A.M. Dirac, *The Principles of Quantum Mechanics* (Clarendon, Oxford University Press, 1958), p. 314
10. C.O. Edet, P.O. Okoi, A.S. Yusuf, P.O. Ushie, P.O. Amadi, Bound state solutions of the generalized shifted Hulthén potential. *Indian J. Phys.* **95**, 471–480 (2021)
11. C.O. Edet, K.O. Okorie, H. Louis, N.A. Nzeata- Ibe, Any 1-state solutions of the Schrodinger equation interacting with Hellmann–Kratzer potential model. *Indian J. Phys.* **94**, 243–251 (2020).
12. C.O. Edet, P.O. Okoi, S.O. Chima, Analytic solutions of the Schrödinger equation with non-central generalized inverse quadratic Yukawa potential. *Rev. Bras. Ensino Fis.* **42**, e20190083 (2020)
13. A.N. Ikot, U. Okorie, A.T. Ngiangia, C.A. Onate, C.O. Edet, I.O. Akpan, P.O. Amadi, Bound state solutions of the Schrödinger equation with energy-dependent molecular Kratzer potential via asymptotic iteration method. *Eclét. Quím. J.* **45**, 65–76 (2020)
14. C.O. Edet, P.O. Amadi, U.S. Okorie, A. Taş, A.N. Ikot, G. Rampho, Solutions of Schrödinger equation and thermal properties of generalized trigonometric Pöschl-Teller potential. *Rev. Mex. Fis.* **66**, 824–839 (2020)
15. C.A. Onate, J.O. Ojonubah, Eigensolutions of the Schrödinger equation with a class of Yukawa potentials via supersymmetric approach. *J. Theor. Appl. Phys.* **10**, 21–26 (2016)
16. M. Hamzavi, K.E. Thylwe, A.A. Rajabi, Approximate bound states solution of the Hellmann potential. *Commun. Theor. Phys.* **60**, 1–8 (2013)
17. A.I. Ahmadov, M. Demirci, S.M. Aslanova, M.F. Mustamin, Arbitrary ℓ -state solutions of the Klein-Gordon equation with the Manning-Rosen plus a Class of Yukawa potentials. *Phys. Lett. A* **384**, 126372 (2020)
18. C.O. Edet, P.O. Amadi, M.C. Onyeaju, U.S. Okorie, R. Sever, G.J. Rampho, H.Y. Abdullah, I.H. Salih, A.N. Ikot, Thermal properties and magnetic susceptibility of Hellmann potential in Aharonov–Bohm (AB) flux and magnetic fields at zero and finite temperatures. *J. Low Temp. Phys.* **202**, 83–105 (2021)
19. G.J. Rampho, A.N. Ikot, C.O. Edet, U.S. Okorie, Energy spectra and thermal properties of diatomic molecules in the presence of magnetic and AB fields with improved Kratzer potential. *Mol. Phys.* **119**, 1–17 (2021)

20. A.N. Ikot, C.O. Edet, P.O. Amadi, U.S. Okorie, G.J. Rampho, H.Y. Abdullah, Thermodynamic properties of Aharonov–Bohm (AB) and magnetic fields with screened Kratzer potential. *Eur. Phys. J. D* **74**, 1–13 (2020)
21. A.N. Ikot, U.S. Okorie, G. Osobonye, P.O. Amadi, C.O. Edet, M.J. Sithole, G.J. Rampho, R. Sever, Superstatistics of Schrödinger equation with pseudo-harmonic potential in external magnetic and Aharonov–Bohm fields. *Heliyon* **6**, e03738 (2020)
22. P. Ghosh, D. Nath, Exact solutions and spectrum analysis of a noncentral potential in the presence of vector potential. *Int. J. Quantum Chem.* **120**, 1–19 (2020)
23. B.T. Mbadjoun, J.M. Ema'a, P.E. Abiama, G.H. Ben-Bolie, P.O. Ateba, Effect of gravity and electromagnetic field on the spectra of cylindrical quantum dots together with AB flux field. *Mod. Phys. Lett. A* **35**, 2050092 (2020)
24. H. Karayer, Study of the radial Schrödinger equation with external magnetic and AB flux fields by the extended Nikiforov–Uvarov method. *Eur. Phys. J. Plus* **135**, 1–10 (2020)
25. N. Ferkous, A. Bounames, 2D Pauli equation with Hulthén potential in the presence of Aharonov–Bohm effect. *Commun. Theor. Phys.* **59**, 679–683 (2013)
26. S.M. Ikhdair, B.J. Falaye, A charged spinless particle in scalar–vector harmonic oscillators with uniform magnetic and Aharonov–Bohm flux fields. *J. Assoc. Arab Univ. Basic Appl. Sci.* **16**, 1–10 (2014)
27. M. Eshghi, H. Mehraban, Study of a 2D charged particle confined by a magnetic and AB flux fields under the radial scalar power potential. *Eur. Phys. J. Plus* **132**, 1–13 (2017)
28. M. Eshghi, H. Mehraban, S.M. Ikhdair, Relativistic Killingbeck energy states under external magnetic fields. *Eur. Phys. J. A* **52**, 1–8 (2016)
29. R. Khordad, M.A. Sadeghzadeh, A.M. Jahan-abad, Effect of magnetic field on internal energy and entropy of a parabolic cylindrical quantum dot. *Theor. Phys.* **59**, 655–660 (2013)
30. P. Kościak, A. Okopińska, Quasi-exact solutions for two interacting electrons in two-dimensional anisotropic dots. *J. Phys. A Math. Theor.* **40**, 1045–1055 (2007)
31. M. Aygun, O. Bayrak, I. Boztosun, Y. Sahin, The energy eigenvalues of the Kratzer potential in the presence of a magnetic field. *Eur. Phys. J. D* **66**, 1–5 (2012)
32. M.K. Elsaid, A. Shaer, E. Hjaz, M.H. Yahya, Impurity effects on the magnetization and magnetic susceptibility of an electron confined in a quantum ring under the presence of an external magnetic field. *Chin. J. Phys.* **64**, 9–17 (2020)
33. S. Gumber, M. Kumar, M. Gambhir, M. Mohan, P.K. Jha, Thermal and magnetic properties of cylindrical quantum dot with asymmetric confinement. *Can. J. Phys.* **93**, 1–5 (2015)
34. R. Khordad, H.R.R. Sedehi, Thermodynamic properties of a double ring-shaped quantum dot at low and high temperatures. *J. Low Temp. Phys.* **190**, 200–212 (2018)
35. R. Khordad, Study of specific heat of quantum pseudodot under magnetic field. *Int. J. Thermophys.* **34**, 1148–1157 (2013)
36. R. Khordad, H. Bahramiyan, H.R.R. Sedehi, Effects of strain, magnetic field and temperature on entropy of a two dimensional GaAs quantum dot under spin–orbit interaction. *Opt. Quantum Electron.* **50**, 1–13 (2018)
37. C.-S. Jia, C.-W. Wang, L.-H. Zhang, X.-L. Peng, H.-M. Tang, J.-Y. Liu, Y. Xiong, R. Zeng, Predictions of entropy for diatomic molecules and gaseous substances. *Chem. Phys. Lett.* **692**, 57–60 (2018)
38. C.-S. Jia, C.-W. Wang, L.-H. Zhang, X.-L. Peng, H.-M. Tang, R. Zeng, Enthalpy of gaseous phosphorus dimer. *Chem. Eng. Sci.* **183**, 26–29 (2018)
39. C.-S. Jia, Y.-T. Wang, L.-S. Wei, C.-W. Wang, X.-L. Peng, L.-H. Zhang, Predictions of entropy and Gibbs energy for carbonyl sulfide. *ACS Omega* **4**, 20000–20004 (2019)
40. J. Wang, C.-S. Jia, C.-J. Li, X.-L. Peng, L.-H. Zhang, J.-Y. Liu, Thermodynamic properties for carbon dioxide. *ACS Omega* **4**, 19193–19198 (2019)
41. C.-S. Jia, J. Li, Y.-S. Liu, X.-L. Peng, X. Jia, L.-H. Zhang, R. Jiang, X.-P. Li, J.-Y. Liu, Y.-L. Zhao, Predictions of thermodynamic properties for hydrogen sulfide. *J. Mol. Liq.* **315**, 113751 (2020)
42. C.-W. Wang, J. Wang, Y.-S. Liu, J. Li, X.-L. Peng, C.-S. Jia, L.-H. Zhang, L.-Z. Yi, J.-Y. Liu, C.-J. Li, X. Jia, Prediction of the ideal-gas thermodynamic properties for water. *J. Mol. Liq.* **321**, 114912 (2021)
43. M. Servatkah, R. Khordad, A. Ghanbari, Accurate prediction of thermodynamic functions of H₂ and LiH using theoretical calculations. *Int. J. Thermophys.* **41**, 37 (2020)
44. M. Eshghi, R. Sever, S.M. Ikhdair, Energy states of the Hulthen plus Coulomb-like potential with position-dependent mass function in external magnetic fields. *Chin. Phys. B* **27**, 020301 (2018)

45. R.L. Greene, C. Aldrich, Variational wave functions for a screened Coulomb potential. *Phys. Rev. A* **14**, 2363–2366 (1976)
46. H. Ciftci, R.L. Hall, N. Saad, Perturbation theory in a framework of iteration methods. *Phys. Lett. A* **340**, 388–396 (2005)
47. B.J. Falaye, Any ℓ -state solutions of the Eckart potential via asymptotic iteration method. *Cent. Eur. J. Phys.* **10**, 960–965 (2012)
48. A. Boumali, The statistical properties of q-deformed Morse potential for some diatomic molecules via Euler–MacLaurin method in one dimension. *J. Math. Chem.* **56**, 1656–1666 (2018)
49. A. Bera, A. Ghosh, M. Ghosh, Analyzing magnetic susceptibility of impurity doped quantum dots in presence of noise. *J. Magn. Magn. Mater.* **484**, 391–402 (2019)
50. C.-S. Jia, L.-H. Zhang, C.-W. Wang, Thermodynamic properties for the lithium dimer. *Chem. Phys. Lett.* **667**, 211–215 (2017)
51. C.-S. Jia, C.-W. Wang, L.-H. Zhang, X.-L. Peng, R. Zeng, X.-T. You, Partition function of improved Tietz oscillators. *Chem. Phys. Lett.* **676**, 150–153 (2017)

Publisher's Note Springer Nature remains neutral with regard to jurisdictional claims in published maps and institutional affiliations.